ENERGY NEUTRAL OPERATION METHOD FOR HYBRID ENERGY STORAGE INTEGRATED WITH WIND FARM USING C-RATE AND FREQUENCY SPECTRUM ANALYSIS

by

Young-Jun Seo

A Thesis Submitted in

Partial Fulfillment of the

Requirements for the Degree of

Master of Science

in Engineering

at

The University of Wisconsin-Milwaukee

May 2015

ProQuest LLC.
789 East Eisenhower Parkway
P.O. Box 1346
Ann Arbor, MI 48106 - 1346

ABSTRACT
ENERGY NEUTRAL OPERATION METHOD FOR HYBRID ENERGY STORAGE INTEGRATED WITH WIND FARM USING C-RATE AND FREQUENCY SPECTRUM ANALYSIS

by

Young-Jun Seo

The University of Wisconsin-Milwaukee, 2015
Under the Supervision of Professor David C. Yu

In this thesis, the author describes various evaluation criteria, in particular the C-rate (charge/discharge-rate), of energy storage (ES) systems to explain the efficiency and technical benefits of battery-ultracapacitor hybrid energy storage (HES), and the technical characteristics of subsequently derived short-duration and long-duration type ES. In addition, for effective use of energy storage, a straightforward state of charge (SOC) correction method for energy neutral operation is proposed, and through a simple comparative example of ES operation, the effectiveness of HES in relation to simple ES is explained. A case is considered in which a hybrid ES controls the wind power ramp rate to comply with the regional system operator's smoothing requirement, and an operation method is suggested through simulation. The simulation is carried out using a frequency spectrum analysis of wind power output profile and the C-rate of the hybrid storage system, and an energy neutral operation method for ES is proposed based on the simulated charging/discharging power sharing profile and SOC variations of the Li-battery and the ultracapacitor .

TABLE OF CONTENTS

LIST OF FIGURES

LIST OF TABLES

ACKNOWLEDGEMENTS

I would like to express my sincerest gratitude to my advisor Prof. David Yu who spared no effort for academic advising, support and guidance in last two years. This thesis would never have been completed without Prof. David Yu's idea. I would also like to thank my thesis committee: Prof. Hossein Hosseini and Prof. Lingfeng Wang for their helpful comments on this work.

I also would like to express my deepest gratitude to my family who always supported me and went through hard times with me.

Chapter 1 Introduction and Literature Review

1.1 Background

For more than a decade, world-wide academic and industrial research has sought to exploit variable energy storage (ES). Various attempts have been made to integrate ES into electric power distribution systems. During this same period, technological advancement have allowed wind energy to become the most economically feasible from of renewable energy. Particularly, as wind farms are becoming larger, wind energy is realizing more and more future energy technologies, which do not emit greenhouse gas, without being depleted. Consequently, energy storage (ES) is drawing more and more attention as a resource that can resolve output intermittency and undispatchability, which are the biggest disadvantages of wind energy. Also because demonstration projects are being extended to commercial operation businesses around the world, ES will be soon used as an important global energy resource.

Investors are able to expect abundant business models with ES connected to the grid. ES units can be typical components for a distributed source, not only supporting a low-voltage distribution system but also supporting a large transmission system. In other words, the applications range from a household using only small appliances to a large steel factory with a load reaching a gigawatt. The extensive range of uses of ES is listed below.

A. Demand Response Resource

Act as a positive or negative generation resource for buildings or factory consumers. The system combined with ES can participate in the demand response (DR) market operated

by independent system operators (ISO). Two DR markets are open separately, which are the reliability DR market (also called emergency DR) and the economic DR market. Usually, the reliability DR market unit bid prices are significantly higher than the economic market. There is a high probability that ES can obtain high profits in the reliability DR market by participating with a thorough strategy.

B. Arbitrage Resource

Buy and sell electricity. ES charges at a low electricity price during the night or on holidays and discharges at a high market price, when electricity loads are high. In this case, ES acts as a pumped hydroelectric power plant. The greater the daily market price differential volatility, the greater profits ES obtains. Furthermore, ES can be operated for the time of use (TOU) electricity rate of the utility, which is for a large-scale customer.

C. Frequency Regulation Ancillary Service

Assist in maintaining electrical frequency (60 Hz). Frequency regulation refers to ancillary service with purpose of managing the quality of energy on the grid. Frequency regulation balances the fluctuations between electricity generation and electrical load. ES absorbs and releases power instantly so that generators connected to the power system can keep rotating at 60 Hz. The deviation between generation and the load is the compensated area control error (ACE) signal, which is calculated from the frequency deviation and tie line MW deviation. The ACE control signal created by ISO can be provided to ES in order to contribute FR. This business model is widely known to have a great value for ES applications, which is profitable with current technology and costs in USA, as well as in South Korea.

D. Spinning Reserve Source

Provide spinning reserve power when the power system lacks reserve. Possible reserves can last 5 to 20 min. The ISO open market for reserves is separate from the energy market.

E. Renewable with ES (Ramp Control and Output Leveling)

Alleviate the intermittency and the irregularity of a wind power plant by rapid charging and discharging of ES. Rather than whole-output leveling, ramp-control using a smaller size of an ESS is more feasible and is widely spreading around the world.

F. Black Start Resource

Provide power for a large generator during start-up when the entire bulk power system is in a black out.

G. Var Compensator

Supply reactive power using converter or inverter reserves in order to control grid voltages. If certain parts of a grid lack reactive power, the voltage will decrease and raise serious problems for electricity quality. The opposite case results in the problem of voltage increase as well.

1.2 Detailed Description of Problems Related to Wind Irregularity

Despite of wind power's many advantages, wind energy's irregularity leads to a variety of problems in a connected power system. Primarily, the voltage fluctuation of a connected grid due to irregular fluctuation of output is a problem. A voltage instability induces a serious problem in stability of power grid and at the same time, has an adverse effect on the life of connected electrical equipment. This irregularity also leads to frequency fluctuation that has adverse effects, in addition to voltage fluctuation.

Frequency fluctuation leads to an adverse effect on the entire synchronized power system. As wind farms and individual wind turbines become larger, wind power makes a more significant contribution to frequency fluctuation.

The frequency fluctuations caused by wind power lead to higher costs required to operate a power system. First, to compensate for the uncertainty of wind power generation, a larger amount of operational spinning reserve must be provided. To satisfy the load of such size, each generator output must be operated at lower than the rated output after turning on many more generators, and consequently, the fuel cost of power generation will be increased. Furthermore, when an additional generator must be deployed owing to imbalanced power generation, a new generator must be one that offers short start-up time and these types are generally more expensive because they require costlier fuels (e.g., diesel and natural gas) compared to generators, such as those based on coal and nuclear power, that require long start-up time. In addition, fluctuations in wind power output make it more difficult for the connected generator to maintain load follow operation, necessitating more frequency-regulating power generation. This leads to harsher conditions related to AGC (automatic generation control) and GF (governor free) operation of a power generator, resulting in reduced generator lifetime and more frequent maintenance. As an example, the cost of ancillary services, including regulation service, accounts for a large proportion—i.e., 3% to 7%—of the total electric bill for the PJM power market.

The intermittency of wind power generation and the resultant voltage fluctuation greatly increase the cost of power system operation. Voltage fluctuation also accelerates the deterioration of connected generators and electrical equipment, and decreases the

quality of the electricity supplied by the power system. To mitigate the voltage fluctuation, an adjacent distribution grid must be reinforced, and further costs are required for installing phase modifying equipment, such as shunt reactors and capacitors, to improve power quality.

The undispatchability of wind power limits its adoption in some regions. Even when the wind resource in region is large, wind power still leads to undesirable effects on the power grid and is thus less feasible than would be expected. This adoption limit increases particularly in an island area. In a region where the connection is weak with main land or an islanded small power system, total power generation cannot depend on wind power because a certain amount of dispatchable power generation satisfying a certain reliability must be maintained. An extreme case is a typhoon, during which the wind speed increases to the point at which wind generation is deactivated, the island must have a contingency plan whereby it can supply power without any contribution from wind generation. Furthermore, some thermal power generators, which can maintain stable frequency, must be secured to a certain extent by assuming that one unit of a large thermal power generator will be tripped because wind power does not have the ability to regulate frequency. In addition, different generators have different ramp up and ramp down characteristics; natural gas generators and hydropower offer fast response, whereas nuclear and coal power have lower ramp rates. Consequently, it is necessary to calculate the wind power generation limit according to the types of generators present in the region. Table 1.1 summarizes the negative effects on a power grid resulting from the intermittency of wind generation.

Problems	Details	Comments
Frequency Fluctuation	-Total power generation cost increases owing to the need to provide additional spinning reserve - Adverse effect on economic dispatch -The harsh conditions of AGC and GF operation lead to reduced generator lifetime and more frequent maintenance	Fuel is more expensive for generators with fast start-up time and high ramp rate
Voltage Fluctuation	-Accelerated deterioration of power generator and installation - Additional distribution grid reinforcement becomes necessary -Additional phase modifying equipment is needed	
Limited Installation Capacity	- Generation cannot rely completely on wind power in a region where the connection with a large power system is weak -The power system must be able to compensate for total deactivation of wind generation -A contingency plan is required to prepare for trip of conventional power generators	A typhoon is an example of a situation that would require emergency power with no contribution from wind generators

Table 1.1 Problems related to wind power intermittency

1.3 Thesis Objectives and Literature Review

Irregular wind power output can be represented in the frequency domain, and its frequency characteristics can be analyzed. This process can be quickly and accurately

carried out using the FFT (fast fourier transform) method. Although it does not focus on ES applications, reference [11] represents wind power fluctuations in the frequency domain and analyzes the frequency deviations in the connected power system. This study suggests that wind power adoption will be limited because of the additional need for frequency regulation in the power grid, and it identifies speed governors as a key component in enabling greater adoption of wind power. This study also includes the formulation of a factor that reflects the increase in ancillary service cost due to wind power, which places higher demands on connected thermal power plants. Reference [1] assumes that the power spectral density of the output of wind turbines provides information on the characteristics of fluctuations in turbine output, and it demonstrates that the spectrum defines the characteristics of the fill-in power that must be provided to compensate for wind power fluctuations when wind generation is deployed on a large scale. Many subsequent studies have investigated wind power fluctuations using a frequency-domain representation. The study of output intermittency via spectral analysis was applied in another field using an ES device, namely, research into HES for plug-in hybrid electric vehicles [2]. In reference [2], a simulation was carried out to reduce the overall cost of hybrid storage following spectral analysis of the electric power output profile characteristics of a plug-in electric vehicle that was repeatedly accelerating and braking. Here, the author carried out a comparative analysis between the performance of an HES system and that of a conventional plug-in hybrid electric vehicle to demonstrate the high power densities and high efficiencies achieved with a lithium-ion battery and an ultracapacitor. Reference [3] investigated frequency sharing between a diesel power generator and a storage system that absorbed the fluctuations of wind generation. The

current profile of the storage system was analyzed based on a frequency-domain representation. The author proposed a method of applying DC and low frequency components to the diesel generator and high frequency components to the battery, and he analyzed the current waveform for the generator and the battery. Several other studies have also investigated wind power fluctuation using spectral analysis techniques.

This thesis presents concepts and techniques that are newer and more detailed than those in the cited references. In this thesis, the author systematically analyzes a role of sharing method for HES systems using frequency spectrum analysis of wind power fluctuations. First, various actively researched storage systems are described and divided into long-duration and short-duration types. Next, the charge/discharge rate (C-rate), a concept used mainly in the conventional battery industry, is defined. To compare a Li battery, Na battery, flow battery, ultracapacitor, and flywheel based on C-rate, which is not used in the ultracapacitor field or the flywheel field, the C-rate is calculated for each device. Based on this comparison, the expected benefits of HES systems are analyzed. Then, after dividing wind power fluctuations into a high frequency region and a low frequency region and assuming that these regions are handled by an ultracapacitor and a Li battery, respectively, a method of determining the borders of the high and low frequency regions using C-rate is described. In this thesis, the method of correcting wind power output using ES is assumed to be ramp control. This was determined based on an example in references [14] and [15], where the maximum ramp rate requirement from the Hawaiian Electric Company (HECO) for First Wind's Kahuku 30 MW wind farm was ±1 MW/min. To adhere to this requirement, First Wind applied a 15 MW / 10 MWh battery from Xtreme Power. In this thesis, the author presents a charging/discharging simulation

assuming that the ramp rate requirement is ±1 MW/min using the 1-minute-interval power generation performance of the existing Samdal 33 MW wind farm in Jeju Province, South Korea. A method is derived to operate the HES cost effectively using C-rate calculations. In addition, the need for energy neutrality, which is an important factor in charging/discharging short-duration ES systems, and a method of maintaining it are introduced. Energy neutrality is an operation method that achieves continuous and symmetrical charging/discharging capability in an ES system by periodically correcting the SOC to 50% by ensuring that the sum of net discharged or charged amounts is zero, taking into consideration the charging/discharging loss.

Chapter 2 C-Rate and ES Technical Characteristics

2.1 ES Evaluation Criteria

Currently, many types of ES are being developed; these include Li batteries, Na batteries, redox flow batteries, ultracapacitors, flywheels, and compressed air ES. All of these systems have completely different technical characteristics, including characteristics related to internal operation and the characteristics of the electrical output. In this thesis, technical evaluation factors are discussed with respect to the power grid of major ES systems, and each ES system is classified according to C-rate, which is the most important factor for determining the proper application for an ES system. The classification of ES systems according to C-rate will be used as a basis for explaining the advantages of HES in Chapter 3.

The evaluation criteria for ES systems participating in the power market are electric output (kW or MW), energy capacity (kWh, MWh, or Ah), and response time (reaction time and ramp rate). Regardless of the type of ES application, the power market provides rewards based only on these three criteria, which can provide a direct profit estimate. Because ES applications with the same rewards can have different internal structures, there are factors to consider in terms of the economic feasibility of an ES application: installation cost, C-rate, life span (cycle life, calendar life), round-trip efficiency, and natural discharging ratio. Unlike other electric performance metrics, the C-rate is very important in ES applications; C-rate will be explained in detail below. Other ES factors that are less important for the power grid but could be important for other applications (for example, transportation or IT equipment) are energy density

(relative to weight or volume), power density (relative to weight or volume), and resistance to vibration and impact. For example, resistance to impact or vibration is far less important for an ES system that is fixed and permanently installed in a power grid application compared to one that is installed in an electric vehicle. Table 2.1 summarizes the evaluation criteria for ES systems.

Factors	Criteria	Comments
Power Market Rewards	- Electric output (MW, kW) - Energy Capacity (kWh, MWh or possible power generation hours) - Response characteristics (ramp rate, reaction time, reaction accuracy)	
Economic feasibility	-Installation cost -Charge/discharge rate (C-rate) -Life span (cycle life, calendar life) -Round-trip efficiency -Natural discharging ratio (or energy conservation ratio)	
Other Factor	-Energy density(relative to weight or volume) -Power density(relative to weight or volume) -Vibration and impact resistance	Possibly important in electric vehicle or IT applications

Table 2.1 Evaluation criteria for ES systems, in relation primarily to power grid applications

2.2 C-Rate and Types of ES

Reference [22] explains that "C-rate is a measure of the rate at which a battery is discharged relative to its maximum capacity." "A 1C rate means that the discharge current will discharge the entire battery in 1 hour." This can be redefined as follows for straightforward application to ES:

$$\text{C-rate of ES } \left[\frac{1}{\text{h}}\right] = \frac{\text{Output Current [A]}}{\text{Current Capacity[Ah]}} = \frac{\text{Inverter or PCS Rated Power [kW]}}{\text{Battery Capacity [kWh]}} = \frac{1}{Operable\ Time\ [h]} \tag{2.1}$$

The C-rate corresponds to the maximum charging or discharging time of the entire energy capacity of an ES system in a specified period of time (namely, 1 hour). Therefore, C-rate can be expressed as a ratio involving inverter rated power or PCS (power conditioning system) rated power, which determines the power in an ES system, and battery capacity or storage capacity, which determines energy. The C-rate is a necessary factor in assessing an ES battery and can also be indirectly calculated for a flywheel ES or an ultracapacitor ES.

If an ES system is charged or discharged at a rate greater than the maximum allowed C-rate, its ES device could be damaged or a fire could result. However, if there is a protection device in the system, this can be activated before damage occurs. The technical characteristics of an ES and its applications according to C-rate must be considered separately. High power ES is appropriate for short-duration applications. That is, a lithium battery (LiB) or ultracapacitor with a C-rate of 1C or higher is suitable for

short-duration applications. Examples of short-duration ES applications are frequency regulation ancillary service, wind power ramp control, and subway regenerative braking. On the other hand, high energy ES systems are useful for long-duration applications. For example, a sodium-sulfur battery (NaS) or redox flow battery (RFB) that slowly charges or discharges at a low C-rate for many hours is suitable for long-duration applications, which include demand response, peak shaving, load leveling, and load shifting. Figure 2.1 depicts the output duration characteristics of ES systems.

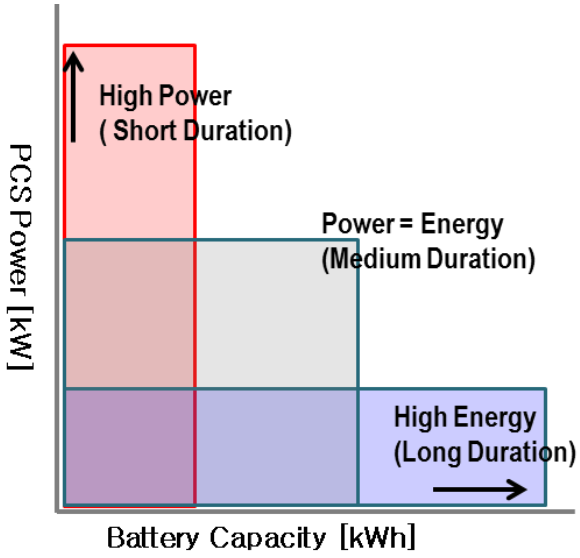

Figure 2.1 Output duration characteristics of ES systems

Of the various ES systems being studied worldwide, this thesis explains the five most promising: LiB, NaS, RFB, ultracapacitor and flywheel.

A. Lithium Battery

With the electrification of transportation, worldwide development of LiBs has accelerated; major manufacturers of these batteries are Samsung SDI, AESC-NEC, Panasonic/Sanyo, LG Chem, GS Yuasa, and Hitachi [18]. These companies have focused

on improving LiB ES because LiBs are suitable for both long- and short-duration applications. Various types of LiBs are available, including lithium manganese oxide (LMO), lithium titanate oxide (LTO), and lithium iron phosphate (LFP). LTO LiBs can provide high C-rates and maximize economic feasibility in short-duration applications requiring minimal battery capacity. Its stability is very high with a long lifetime, and its DC-to-DC efficiency reaches approximately 97%. LMO LiBs are reasonably priced owing to mass production and are appropriate for electric vehicle batteries and other long-duration applications; the LiB ES which is also available for family use small scale some ES cannot be small, compared to many other battery ES system, is widely used in the world.

B. NaS[17]

Sodium-sulfur batteries, for which Japan possesses leading technology, are promising devices for future ES systems because they offer high energy density relative to production cost. With current technology, these batteries can function only when Na is in a liquid state, and this requires a high internal operation temperature of 300°C. That is, the system requires daily charging and discharging to maintain the melting condition. If operation stops, the inside becomes completely solidified only after three days, and re-operation requires a 12hours warm-up, which impedes good efficiency. This operation temperature makes size reduction difficult and leads to safety concerns and low overall efficiency; consequently, applications for sodium-sulfur batteries are currently limited. Because of its extremely low C-rate of approximately 1/6C, NaS is inappropriate for a short duration application. Despite its many weaknesses, its strengths are economic cost, high energy density, and easy mass storage.

C. RFB

The potential difference of two chemical components dissolved in liquids charges and discharges electrical energy while the electrolyte in the tank flows through the membrane. The output power is about 0.5C and the efficiency of the round-trip DC is also belong to the low side, approximately 70%. However, its lifetime is long, and it is good for mass storage at a low cost..

D. Ultracapacitor

Based on the basic principle of the condenser, UC stores electrical energy without chemical reactions and has a semipermanent lifespan. Because of its excellent short-duration operation, its C-rate reaches over 200C, allowing it to charge and discharge with a momentary high output. However, it is inappropriate for large storage and only good for a short-duration application.

E. Flywheel

Electrical energy is converted to rotational kinetic energy for storage. Its installation cost is higher than other ES systems, and the energy density is low. As a rotational machine, its maintenance and repair cost is high. Also it has a very high self-discharge rate. However, it charges and discharges with a high output, which is suitable for short-duration applications, and its lifespan is semipermanent.

Table 2.2 and 2.3 show technical characteristics and estimated actual prices for various ES systems. The author has tried to provide ES cost and C-rate data based on published information. However, some of these data, including those for the newest industrial technologies, are based on oral information gathered during the author's practical work experience in national ES research and development projects in S. Korea.

ES type	Required Energy for 1MW PCS	C-rate	Cost [$/MWh]	Comments
LMO	0.5MWh	2C	1m$[A]	Lithium manganese oxide: typical Li-Battery
LFP	0.25MWh	4C	1.5m$	Lithium iron phosphate
LTO	0.2MWh	5C~6C	3m$	Lithium titanate oxide
NaS	6MWh	0.17C	0.25m$	From Reference [17]
RFB	2MWh	0.5C	0.6m$	
UC (EDLC)	5[kWh]	200C[B]	20m$	EDLC system specifications from reference [16] -Rated voltage : 583.2[V] -Rated current : 1200[A] -Rated capacity : 10.5[MJ] or 3[kWh] C-rate = 583.2 × 1,200/3,000 = 233
Flywheel	0.25MWh	4C[B]	15m$	From the Beacon Power 20MW Smart Energy Matrix – Stephentown, NY -Rated power : 20MW -Operable time : 15min or 5MWh C-rate = 20/5 = 4

Table 2.2 C-rate for various ES systems

[A] m$ = millions of US dollars.

[B] For C-rate comparison among various ES systems, a database can be constructed using approximate values estimated indirectly through examples of system specifications for actual projects, and the database can be updated according to developments in the relevant technology.

ES type	LMO	LTO	LFP	NaS [17]	RFB	UC [16]	Flywheel
Maker	Samsung SDI, Panasonic/ Sanyo LG-chem, SK-Inno.	Kokam, Tosiba	BYD	NGK	Prudent Energy. ZBB, Lotte-chem	Panasonic, NCC, Maxwell	Beacon Power
Cell Voltage	3.7V	2.4V	3.2V	1.9V	1.2-1.8V	2.7V	-
Life (Cycle/Calendar)	1,500 10years	9,000 20years	4,000 -	4,000 15years	2,000-5,000 10years	Semiper manent	Semiper manent
DC Efficiency	97%	-	-	85%	70%	85-95%	90%
Self Discharge	5-10%/ month	-	-	Almost 0%	5-10%/ month	Very High	Very High
Low Temp. Performance	Better	Best (-50℃)	Good	-	-	-	-
Application	FR, RC, LL, PC, Arbitrage	FR, RC	FR, RC	LL, PC, Arbitrage	LL, PC, Arbitrage	FR, Subway Regenerative Breaking	FR

Table 2.3 Technical characteristics of ES

Abbreviations: FR (frequency regulation), RC (ramp control of wind power), LL (load leveling), PC (peak cut)

Consequently, sources are not identified for all of the information in the table. Additionally, because current technologies and markets related to ES are not mature, some of the data presented in this thesis may not be completely accurate. In addition, some of the numerical values presented in this thesis are estimated based on data from multiple sources. For the performance analysis, the C-rates of ES systems that are not battery based (i.e., flywheel and ultracapacitor systems) are indirectly calculated according to published specifications. As is evident in Table 2.2, a reciprocal relationship exists between the "Required Energy for 1 MW PCS" values and the C-rate values.

When a large amount of power is produced for a short time such that the C-rate of an ES system is exceeded, either the output will be limited to less than the desired output by physical mechanisms or chemical reaction rates, or the system will incur damage. C-rate is the most important factor for commercial applications because it has the largest influence on the characteristics of the electrical output of an ES. It is difficult to find C-rate data from ES system manufacturers because the maximum allowable C-rate may vary according to different operation conditions. For example, in the case of lead-acid batteries, which are frequently used in automobiles, the capacity is calculated on the basis of a fixed C-rate (usually 0.2C). For a 12 V, 50 Ah battery, the 50 Ah (0.6 kWh) will be exhausted only if the battery is used at 0.2C for 5 hours. However, in the case of faster discharging with higher current—for example, when supplying an automobile starter motor that consumes 2 kW—the energy supplied by the fully charged battery is less than 0.6 kWh. This is because the battery is used at 3.3C (2 kW/0.6 kWh). Typical discharge curves for lead-acid batteries as a function of C-rate are found in [21]. Thus, we can indirectly estimate the maximum allowable C-rate for the ES, which is stable

even when operated for a long period of time, based on the ratio between the capacity of the PCS and that of the battery.

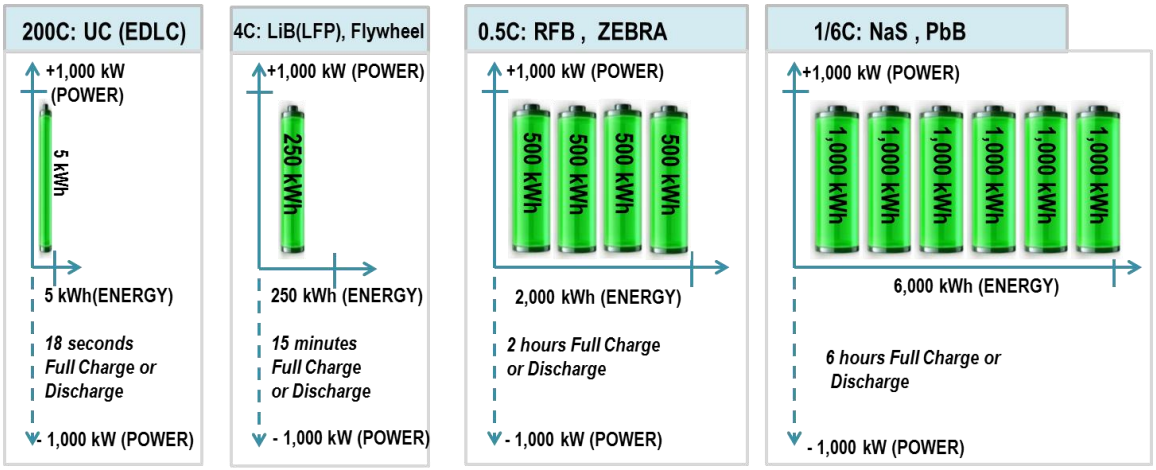

Figure 2.2 C-rates and full charge or discharge durations of various ES systems

Abbreviations for Table 2.2 and Fig. 2.2: UC, ultracapacitor; EDLC, electric double layer capacitor; LiB, lithium battery; ZEBRA, Zeolite Battery Research Africa project; NaS, sodium-sulfur battery; PbB, lead-acid battery.

Figure 2.2 illustrates the concept of C-rate and provides specific C-rate information for major ES systems. For example, if an ES system produces a rated output of 1 MW, a 0.25 MWh battery is sufficient if a 4C LiB is used. However, if 0.5C RFB is used, a battery of at least 2 MWh capacity is required.

2.3 SOC Correction and Energy Neutral Operation

The SOC (state of charge, i.e., percentage of battery charge) continuously changes in an ES that is being charged and discharged for a wind power intermittency or power system frequency regulation application. If the energy input and energy output of an ES are not properly balanced, a battery will enter a full charge (FC) or complete discharge (CD) state, and symmetric regulation cannot be maintained. The maximum performance of an

ES can be achieved with minimal battery capacity only if the SOC is corrected to 50%. In other words, if the energy charge and discharge except all losses are periodically balanced, the battery is in energy neutral operation, and the continuous charging range and discharging range can be maintained symmetrically. Operation with continuous charge/discharge repeating is very important and greatly facilitates maximizing efficiency while minimizing battery capacity. The energy neutral condition is expressed as follows:

$$\int_0^D (P_{charged}(t) - P_{discharge}(t))dt = 0 \tag{2.2}$$

where D is a duration that varies according to the SOC correction intensity factor (CIF).

Figure 2.3 shows the output of an existing 33 MW wind farm. As a simple example, it is assumed that the ES system seeks flat power leveling based on an average output. In real-life situations, perfectly flat power leveling is rarely necessary; controlling

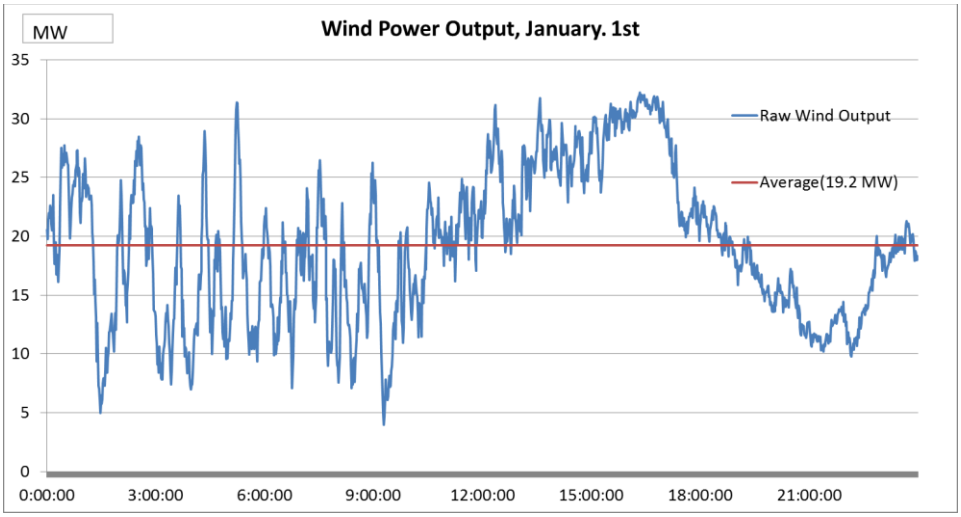

Figure 2.3 One-minute-interval raw wind output and the average output used for power leveling

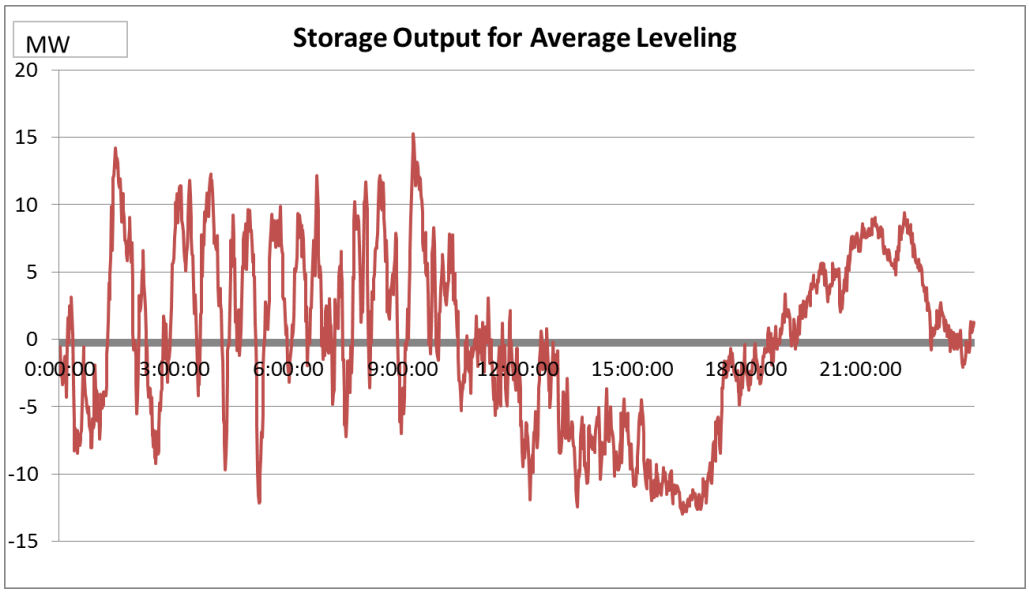

Figure 2.4 Output of the ES system for power leveling

ramp rate to less than several MW/min is generally sufficient. In this case, though, ideally flat power leveling is assumed in order to aid understanding. The regulation output of an ES system for perfectly flat leveling control is shown in Fig. 2.4, with the assumptions that the PCS rated power and the C-rate of the ES system are sufficient.

If the raw wind output in Fig. 2.3 is denoted by P_W, the average power of the raw wind output by P_{Ave} (set as a correction target value to 19.2 MW), and the ES output in Fig. 2.4 by P_{ES}, then

$$P_{Ave}(\mathrm{t}) = 19.2\mathrm{MW} = P_W(\mathrm{t}) + P_{ES}(\mathrm{t}) \tag{2.3}$$

If it is assumed that a battery of approximately 10 MWh capacity is applied, the SOC varies as shown in Fig. 2.5. Again, the PCS rated power and the C-rate of the battery are assumed to be sufficiently large and thus are ignored.

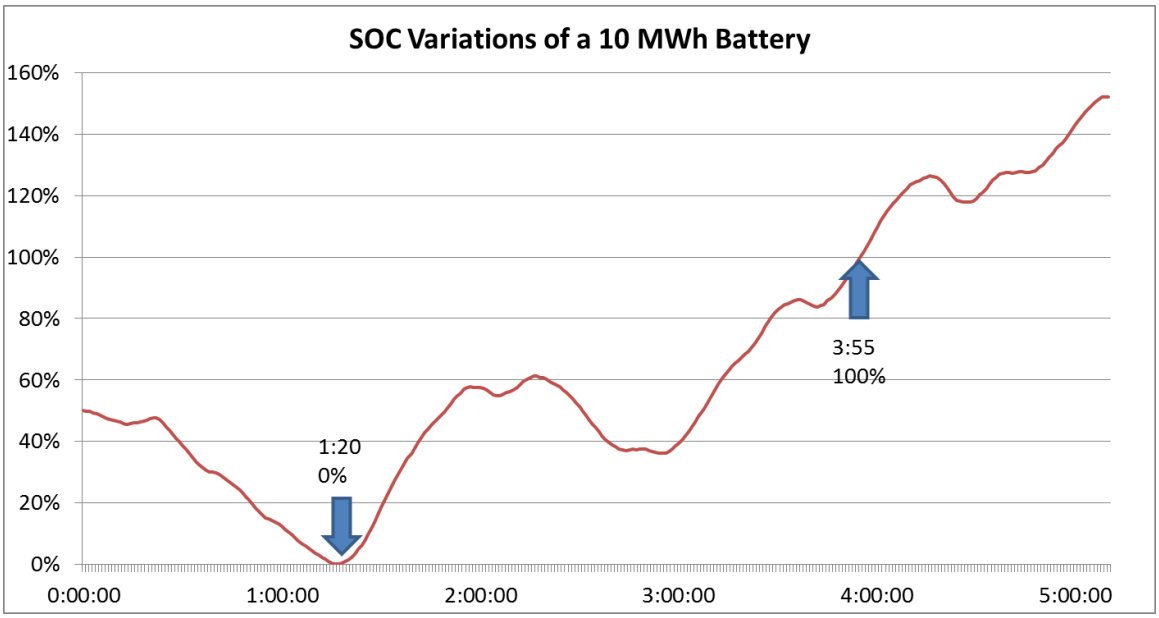

Figure 2.5 SOC variations of a 10 MWh battery

The SOC in Fig. 2.5 is expressed as

$$SOC(t) = SOC(t - 1\ \text{min}) - \frac{P_{ES}(t)}{60} \times \frac{1}{E_{ES}} \tag{2.4}$$

where $P_{ES}(t)$ is the storage output and E_{ES} is the rated storage capacity. When regulation for power leveling is initiated, the SOC is 50%, and after 1 h 20 min, the storage system reaches the CD state. At 3 h 55 min, the SOC reaches and then exceeds the FC state. In a real-life situation, the SOC cannot exceed 100% or fall below 0%. As shown in the simulation results in Fig. 2.4, when the system is in a CD or FC state, symmetric regulation cannot be maintained. That is, regardless of the leveling target, only charging with no discharging is possible in the CD state and only discharging with no charging is possible in the FC state. To prevent these conditions, the SOC must be periodically corrected to 50%.

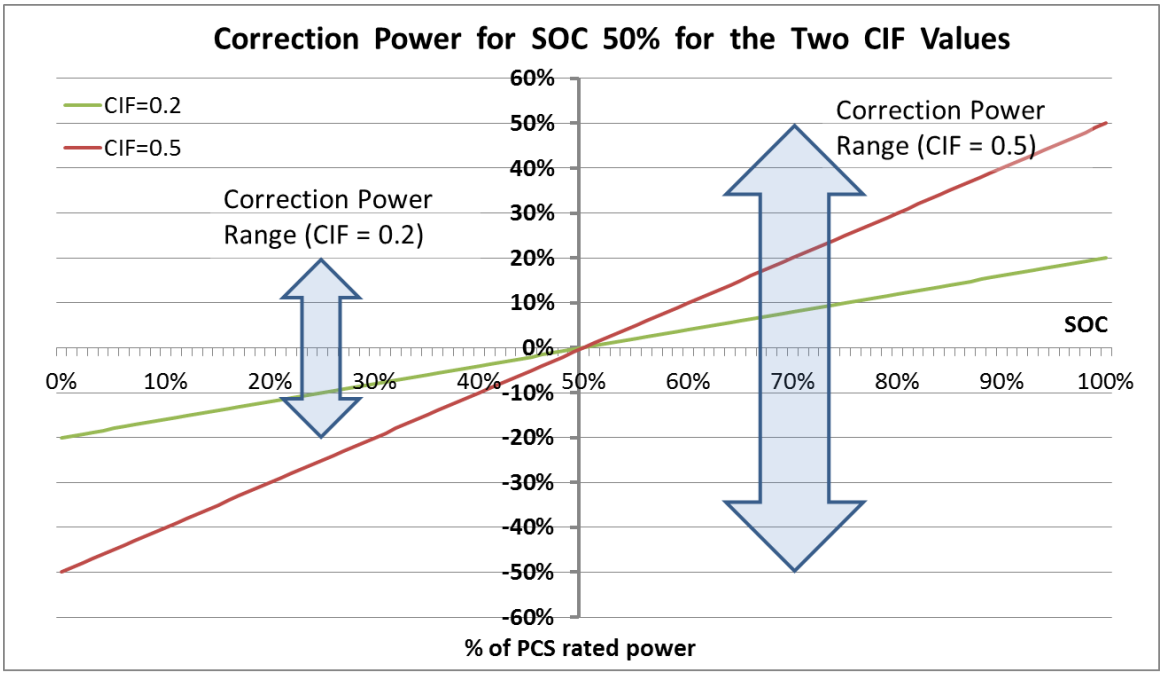

Figure 2.6 SOC correction power with correction intensity factor (CIF) of 0.2 and 0.5

Figure 2.6 presents an example of simple correction control for correcting the SOC to 50%. This method produces a maximum correction output at 0% SOC (CD) or 100% SOC (FC), that is, where the deviation from 50% SOC is maximized. Figure 2.6 includes cases in which the maximum correction output is set to 20% or 50% of the PCS rated power. The correction output power P_{COR} shown in Fig. 2.6 is expressed as follows:

$$P_{COR}(t) = P_{ES} \times (2CIF \times SOC(t) - CIF) = P_{ES} \times CIF \times (2SOC(t) - 1) \quad (2.5)$$

where CIF is the correction intensity factor expressed as a proportion of the PCS rated power. In other words, if the CIF is set to 0.5 and the PCS rated power is 10 MW, the correction targets are 5 MW discharging output in the FC state and -5 MW charging output in the CD state. Here, with higher CIF, the flat power leveling effect on the wind

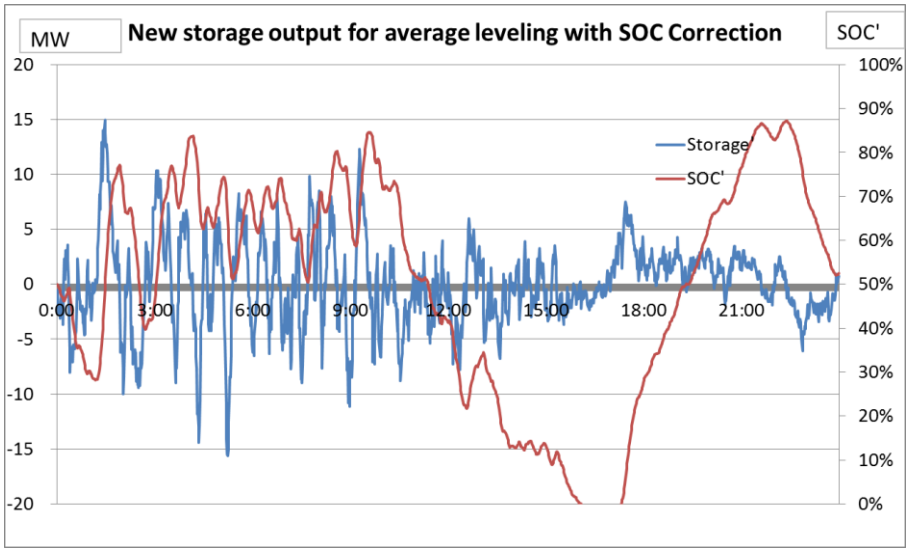

Figure 2.7 Output of the ES system and SOC variations after implementing SOC correction control

output, which is the original goal of the ES system, is reduced. However, with higher CIF the consumed battery capacity can be minimized. This method also has a limitation

related to C-rate—that is, only if the C-rate of the battery is sufficiently high can the battery capacity be reduced when a higher CIF is used.

Figure 2.7 shows the ES output and the SOC variations after incorporating SOC corrections into the ES system. Compared to the results in Fig. 2.5, the deviation of SOC is significantly reduced and less imbalanced. This is because the correction target of 50% SOC was applied to the flat power leveling target for the wind output. The SOC is not continuously biased toward the positive direction or the negative direction, and an energy neutral characteristic is evident in that the SOC periodically passes through the 50% level.

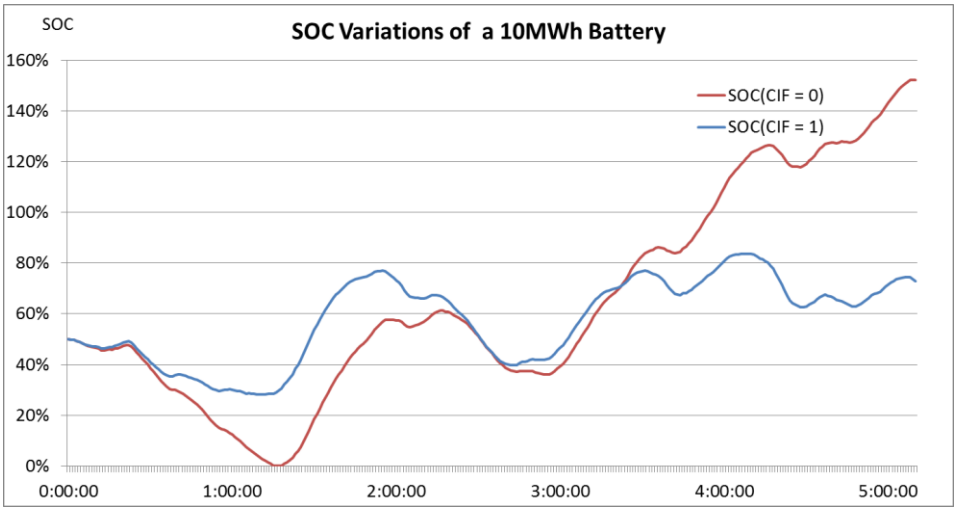

Figure 2.8 Comparison of SOC variations with CIF = 1 and CIF = 0

Two cases of SOC variations are shown in Fig. 2.8. The SOC is more stable when CIF = 1. A stable CIF facilitates energy neutral operation and allows a proper ES capacity to be selected.

Fig. 2.9 shows total system output according the CIF values. Total system output is a value obtained by adding wind output and ES system output. Prior to carrying out the SOC correction, total output is "average (CIF=0)" of Fig. 2.8. However, after the SOC correction, the total output changes to "After SOC correction (CIF=1)".

$$P_{total}(t) = P_W(t) + P_{ES}(t) + P_{COR}(t) \tag{2.6}$$

When SOC correction is performed, it is possible to implement changes that also negatively affect the targeted total system output. Regarding the goal of ES with respect to realistic wind power intermittency, because controlling ramp rate to less than several MW/min (as opposed to perfectly flat power leveling) is sufficient, the total system output after SOC correction shown in Fig. 2.9 represents sufficient improvement in wind

power output quality. In realistic circumstances, however, the battery capacity cannot be increased infinitely, and thus it is necessary to adjust the CIF value according to the desired battery capacity. The CIF value can be set from 0 to values larger than 1; an additional optimization study would be necessary to analyze the effects of CIF values larger than 1.

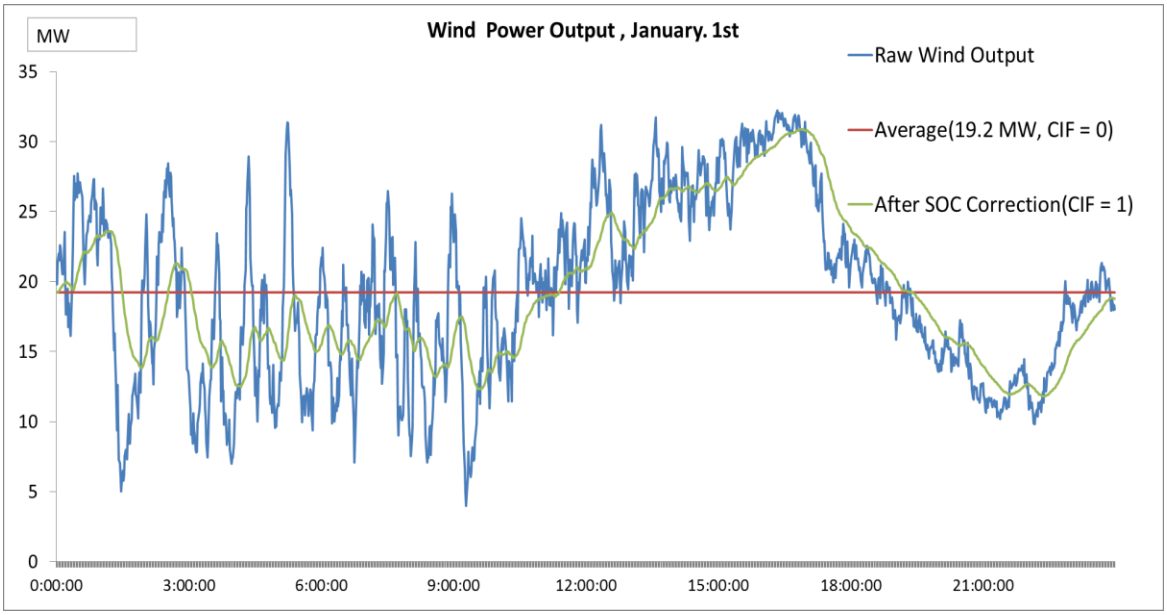

Figure 2.9 Total system output for CIF = 0 and CIF = 1

Chapter 3 Effectiveness of Hybrid ES in Comparison with Simple ES

To demonstrate the benefits of HES, a simple simulation can be carried out to examine the efficiency of a simple energy storage (SES) system relative to that of an HES system. An SES system consists of only one storage device, whereas an HES system incorporates two ES devices with different characteristics. Figure 3.1 presents an example of an output target for an ES system.

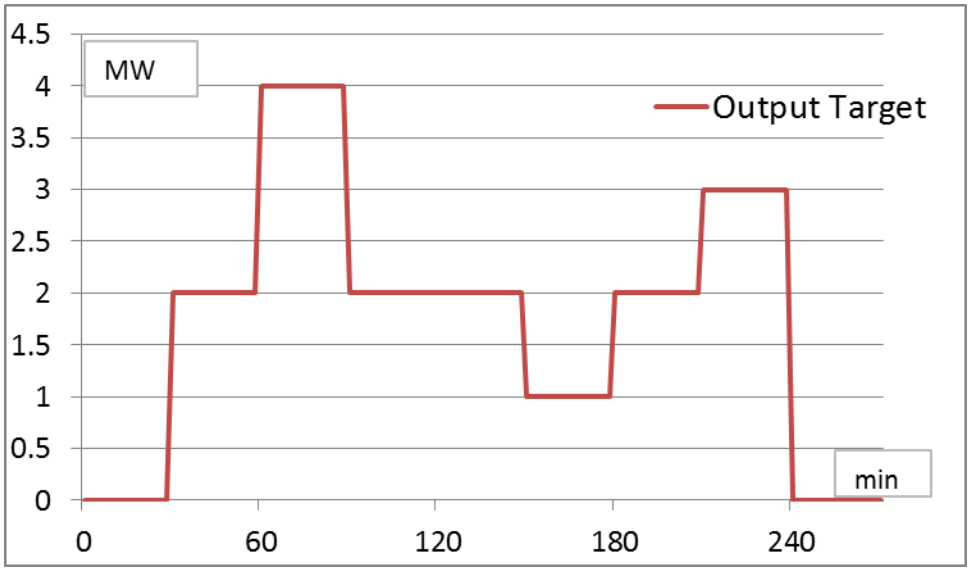

Figure 3.1 Example of an output target for an ES system (power output range of 1 MW to 4 MW, with total output energy of 8 MWh)

As shown in Fig. 3.1, the system starts to produce 2 MW output at 30 min and must supply a total of 8 MWh of energy with power between 1 and 4 MW for 3 h 30 min. If it is assumed that an SES system is implemented with only an LiB (LMO, 2C) to satisfy the above output target, an LiB of 8 MWh capacity is adequate because the C-rate of the LiB is sufficiently high: the maximum allowable C-rate of the LiB is 2C, and as a result the 0.5C system consisting of a 4 MW PCS and an 8 MWh LiB will not experience

problems. In other words, when an LiB SES system is implemented, the most economical system is one with a 4 MW PCS and an 8 MWh battery. The cost of the PCS is approximately 0.3 m$/MW and (according to Table 2.2) that of the LiB is 1 m$/MWh, and thus the total cost is calculated simply as follows:

$$\text{PCS}\ (0.3\text{m\$} \times 4\text{MW}) + \text{Battery}\ (1\text{m\$} \times 8\text{MWh}) = 9.2m\$ \tag{3.1}$$

If the SES system is implemented using an NaS, one must be careful when choosing the battery capacity because the NaS has a lower maximum allowable C-rate. If an 8 MWh NaS is used to produce an output of 4 MW maximum, the C-rate must be at least 0.5C. This exceeds 0.17C, the maximum allowable C-rate of sodium-sulfur batteries as given in Table 2.2. Thus, this design could result in a damaged battery or a fire. The minimum NaS capacity needed for an output power of 4 MW is determined as follows:

$$\frac{4MW}{0.17C} = 23.5MWh \tag{3.2}$$

The cost of this NaS SES system is the following:

$$\text{PCS}\ (0.3\text{m\$} \times 4\text{MW}) + \text{Battery}\ (0.25\text{m\$} \times 23.5\text{MWh}) = 7.1m\$ \tag{3.3}$$

Now an HES system consisting of an LiB and an NaS will be considered. The respective outputs of two ES systems having different characteristics can be controlled as shown in Fig. 3.2.

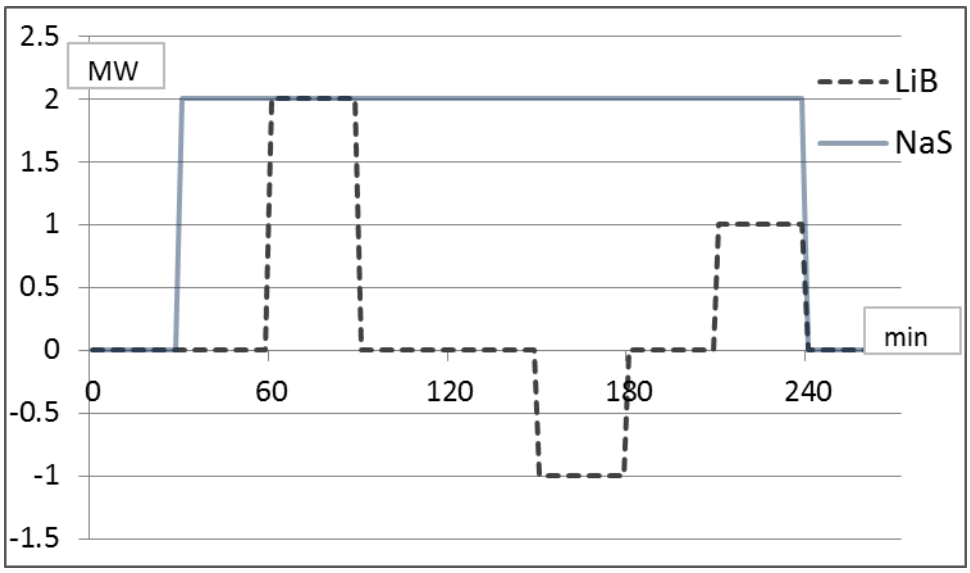

Figure 3.2 Example of an output combination for satisfying the output target in an HES consisting of an LiB and a NaS

The output profiles shown in Fig. 3.2 demonstrate how the outputs of two ES systems can be added to obtain an output that satisfies the target. A positive output corresponds to discharge, and a negative output corresponds to charge. The output combination in Fig. 3.2 is merely an example; various output combinations can be designed according to the technical characteristics and usage of the ES system. In the output profile of Fig. 3.2, the LiB must be able to produce 1 MWh of energy within a power output range of -1 MW to 2 MW. The NaS must be able to produce 7 MWh of energy at 2 MW of output power. The LiB system (with maximum allowable C-rate of 2C) will be adequate with a 2 MW PCS and a 1 MWh battery. The NaS, however, cannot produce 2 MW of power with a 7 MWh capacity owing to a lower C-rate. A battery capacity of at least 11.7 MWh (2 MW/0.17C) is required.

The cost of the LiB storage system is as follows:

$$\text{PCS}\ (0.3\text{m\$} \times 2\text{MW}) + \text{Li Battery}\ (1\text{m\$} \times 1\text{MWh}) = 1.6m\$ \quad (3.4)$$

The cost of the NaS storage system is as follows:

$$\text{PCS}\ (0.3\text{m\$} \times 2\text{MW}) + \text{NaS Battery}\ (0.25\text{m\$} \times 11.7\text{MWh}) = 3.5m\$ \quad (3.5)$$

The total cost of the hybrid system is thus

$$\text{LiB system}\ (1.6\text{m\$}) + \text{NaS system}\ (3.5\text{m\$}) = 5.1m\$ \quad (3.6)$$

Table 3.1 compares the costs of the three ES systems..

ES type		**Calculated Cost**
Simple Energy Storage	LiB	9.2m$
	NaS	7.1m$
Hybrid Energy Storage	LiB+NaS	5.1m$

Table 3.1 Cost comparison of three ES systems that satisfy the output target

Characteristics other than C-rate, such as cycle life, efficiency, and operation temperature, should also be considered in ES system design. C-rate, however, is the most important factor, and this chapter has demonstrated that when only C-rate is considered, HES systems can be more economical than SES systems. In other words, it is possible to design an ES system with adequate performance and lower cost by employing a combination of storage types with different C-rate characteristics.

Chapter 4 Operation Simulation for Wind Power Ramp Control

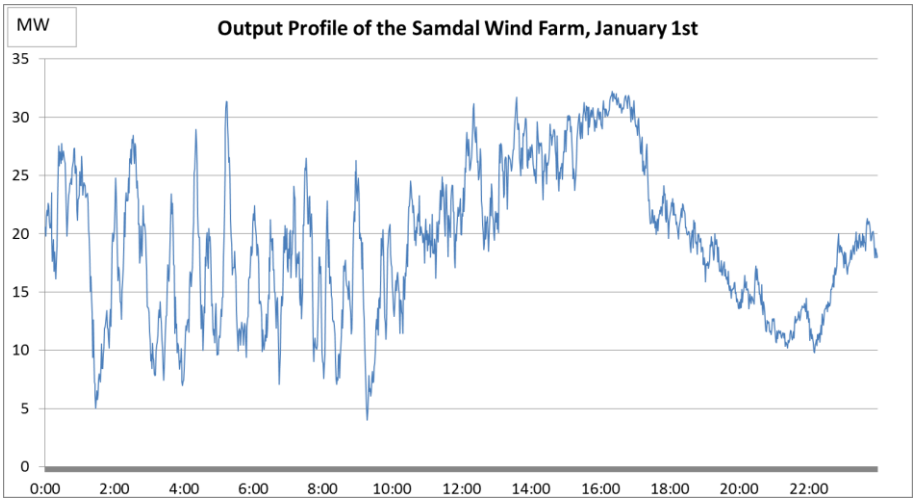

Figure 4.1 One-min-interval output profile for the 33 MW Samdal Wind Farm in Jeju Province, South Korea

The 1-min-interval output profile of the 33 MW Samdal Wind Farm in Jeju Province, South Korea (see Fig. 4.1), was used to simulate wind power ramp control with an HES system. References [14] and [15] discuss actual cases in which 15 MW/10 MWh ES was applied to control the ramp rate of the 30 MW Kahuku wind farm to less than ±1 MW/min.

The HECO ramp rate requirement for Kahuku Wind Power (KWP) is shown in Fig. 4.2. Reference [15] states, "HECO requires limits on maximum allowed ramp rates (MW/min); defines voltage and frequency ride-through characteristics; and sets power quality, voltage regulation, and active power control requirements." "The KWP power purchase agreement was negotiated in 2008 and includes different upward and downward ramp interconnection requirements that vary depending on the time of the day."

The operation characteristics of the HES system are analyzed assuming that an ultracapacitor and an LiB are used; these two devices have significantly different C-rates.

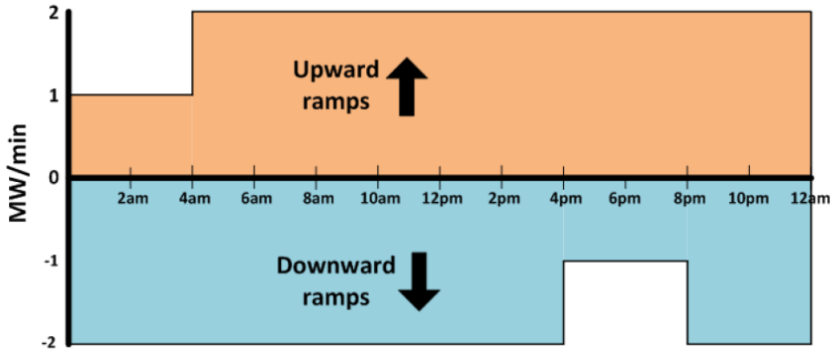

Figure 4.2 HECO ramp rate requirement for the Kahuku wind farm [15]

Many researchers have analyzed wind power output by converting it into the frequency domain, often by means of the convenient and straightforward FFT technique [1], [5], [7], [8], [11], [12]. In this thesis, wind power output in relation to C-rate is analyzed using the FFT, and in addition simulations are carried out to investigate the effects of SOC correction. Furthermore, this thesis makes a small contribution to this field of study by proposing a simulation technique for operation methods based on HES using two devices with different C-rates. In the ultracapacitor or supercapacitor industry, the specification referred to as C-rate is not used. The author thinks that this is because C-rate originates from the battery industry, specifically the lead-acid battery industry. Typically, the capacity of an ultracapacitor is expressed in farads (F) or joules (J) instead of watts (W) or ampere-hours (Ah). However, the development of hybrid storage systems, in which two or more ES types are combined, is increasingly important. Thus, there is need for a specification such as C-rate that can apply to batteries, capacitors, flywheels, superconducting magnetic ES, and compressed air ES. If it is eventually decided that C-rate is not suitable for the various ES systems, it would be simple to replace it with a specification, such as P-rate (power rate) or E-rate (energy rate), that can be used throughout the ES industry.

Fortunately, farads and joules can be easily converted to watts, and thus the C-rate of an ultracapacitor can be calculated. The C-rate of a flywheel can be indirectly determined using a operable time offered by the manufacturer or the business operator. For example, for a 20 MW/15 min flywheel, the C-rate can be calculated as 4C using Eq. (2.1), and this value can be incorporated into an analysis of the components of an HES. When an HES system employs devices with different C-rates, simpler and clearer operation and sizing are possible. Table 4.1 lists the C-rates and costs of HES components.

ES Type		**C-Rate**	**Cost**	**Required Energy Capacity For 1MW PCS**
Hybrid Energy Storage	LiB (LMO)	2C	1 m$/MWh	0.5 MWh
	Ultracapacitor [16]	200C	20 m$/MWh	5 kWh
	PCS	-	0.3 m$/MW	-

Table 4.1 C-rates and costs of HES components

4.1 Frequency Spectrum of the Wind Power Profile

The result of the FFT can be used to represent the magnitude of the frequency contents at various frequencies and that is complex vector representing the magnitude and phase data[24]. In Fig. 4.3, each bar shows only absolute value excluding the phase of cosine wave for each frequency. Frequency with the most power was the frequency of zero. This represents nothing but the constant offset. The large spike of zero frequency makes it difficult to observe the other relevant frequencies[24].

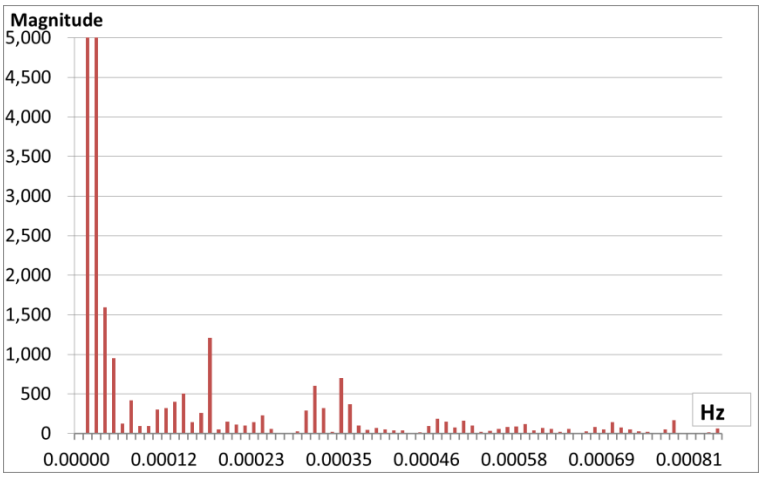

Figure 4.3 FFT results for the wind farm power output

Therefore, the FFT result of Fig. 4.3 is the result after subtracting the average value from the wind power FFT value itself to eliminate the zero frequency spike.

The wind power sampling interval (Ts) is 60 s. Therefore, the total FFT spectrum range is:

$$\frac{F_S}{2} = \frac{1}{2T_S} = \frac{1}{2\times 60sec} = 0.0083Hz \tag{4.1}$$

In the above equation, the sampling frequency (FS) is divided by 2 because this corresponds to the Nyquist frequency. The result of the FFT is valid only from 0 Hz to the Nyquist frequency. Beyond this frequency, the FFT results repeat themselves [24]. Therefore, a half of FFT figure is a mirror image by redundancy.

Figure 4.4 shows the frequency spectrum of the intermittent wind power output divided into three sections corresponding to the use of the ultracapacitor and the LiB in the HES system. The vertical axis on the right side represents the accumulated magnitude

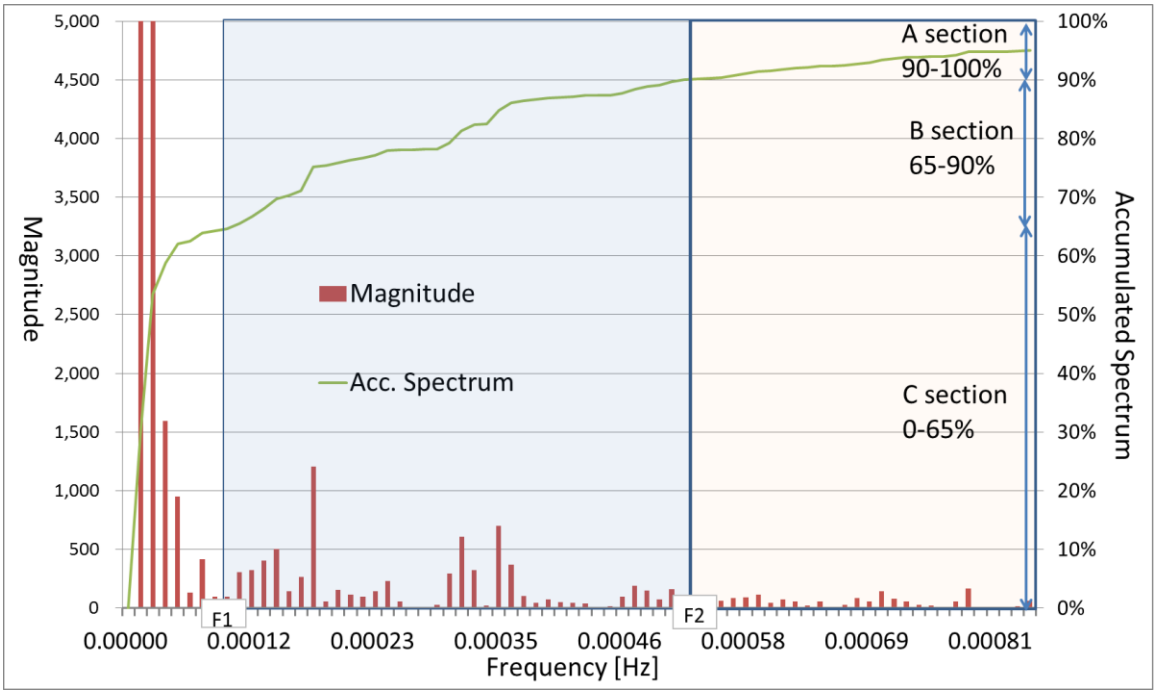

Figure 4.4 FFT data for the wind farm output, divided into three sections

relative to the total magnitude of all frequency components included in the graph. Three frequency sections are defined based on frequencies corresponding to a certain accumulated magnitude. The A section includes frequencies for which the accumulated magnitude is from 90% to 100% of the total magnitude; this section is handled by the ultracapacitor. The border frequency F2 is approximately 0.00053 Hz. The B section includes frequencies for which the accumulated magnitude is from 65% to 90%; it is handled by the LiB. The border frequency F1 is approximately 0.00009 Hz. The C section includes the lowest frequencies, with accumulated magnitude from 0% to 65%. In this section, the ramp rate of the wind power fluctuation is lowest, corresponding to relatively mild fluctuation. In other words, the C section represents Ptotal(t), that is, the total system power generation output, which is supplied to the power system through the point of common coupling or PCC.

A formula for filtering the 1-min-interval wind power profile is the following:

$$FV = PFV + (CIV - FV) \times \frac{CT-PT}{TC} \times \left(1 - \left(0.25 \times \frac{CT-PT}{TC}\right)\right) \quad (4.2)$$

where FV stands for filtered value, PFV for previous filtered value, CIV for current input value, CT for current time, PT for previous time, and TC for time constant.

The border frequencies for the three sections are calculated as follows:

$$F_C = \frac{1}{2\pi TC} \quad (4.3)$$

4.2 Charge and Discharge Coordination for Hybrid ES

Figure 4.5 presents a time domain plot for the A section, which is handled by the ultracapacitor. Figure 4.6 presents a plot for the B section, which is handled by the LiB. The time axis starts at 01:00 in Figs. 4.5 and 4.6 because the filtered values generated by the low-pass filter (Eq. (4.2)) include inaccurate transients during the initial period. Thus, the data from 0 to 59 min were omitted to allow for an accurate analysis. As is apparent, the frequencies in the A section plot are higher. Because charging/discharging is repeated more frequently in the A section than in the B section, it can be predicted that the one-round-trip energy will be smaller. It is thus appropriate to use the ultracapacitor, which offers high C-rate with low energy capacity. The overall magnitude of the charge/discharge power is similar in the plots for the B section and the A section, but the lower frequencies in the B section indicate that the round-trip energy is higher. Figure 4.7 presents a plot of the total system output of the HES system after correction. The mild

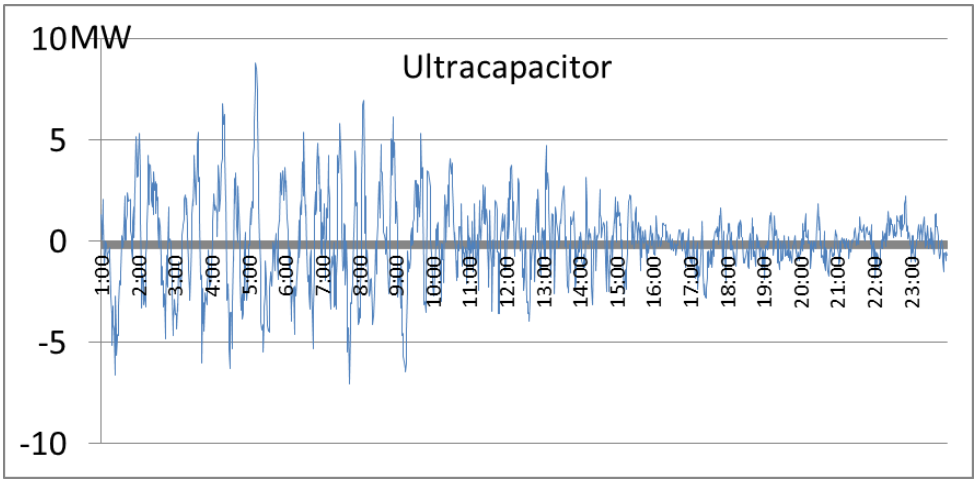

Figure 4.5 Time domain plot for the A section of the wind farm output frequencies

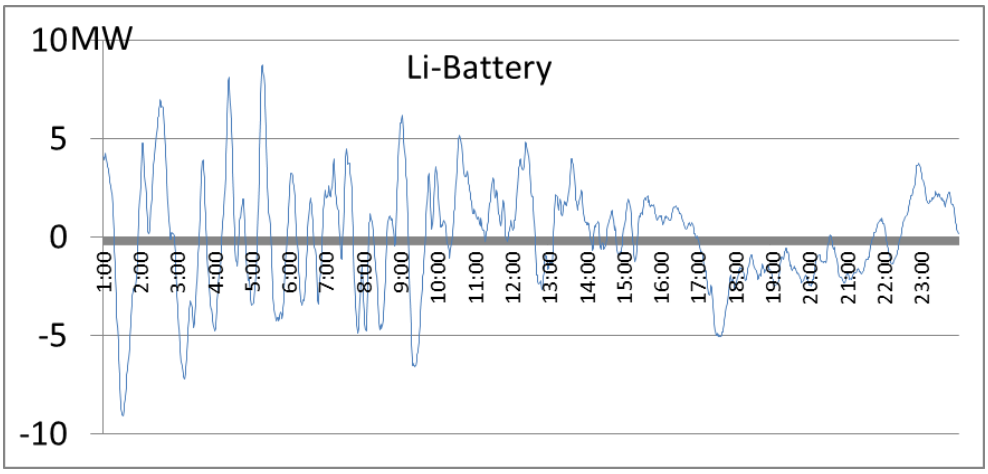

Figure 4.6 Time domain plot for the B section of the wind farm output frequencies

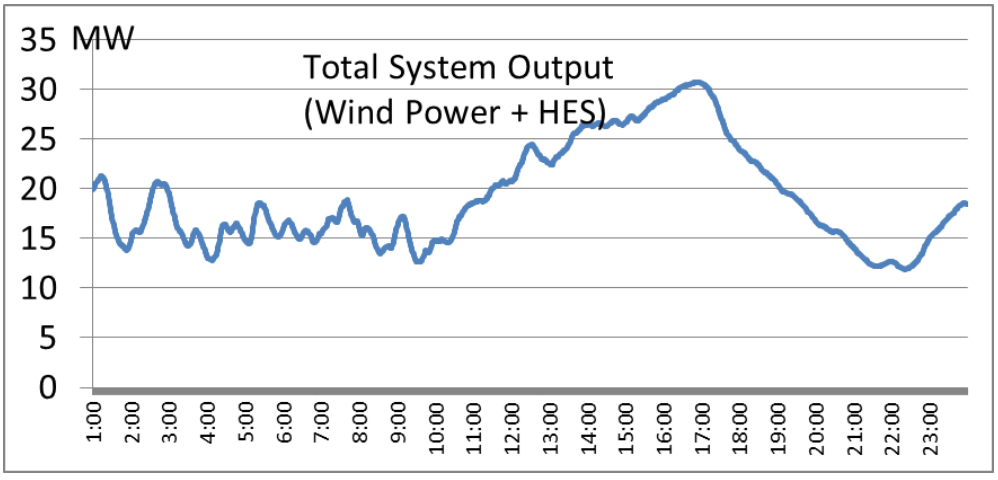

Figure 4.7 Time domain plot for the C section of the wind farm output frequencies

fluctuations depicted in this plot can adequately resolve the problems caused by wind irregularity described in section 2 of chapter 1. As shown in Fig. 4.5, the maximum output of the A section is approximately 8 MW, and thus the storage system can be designed with an 8 MW PCS and an ultracapacitor.

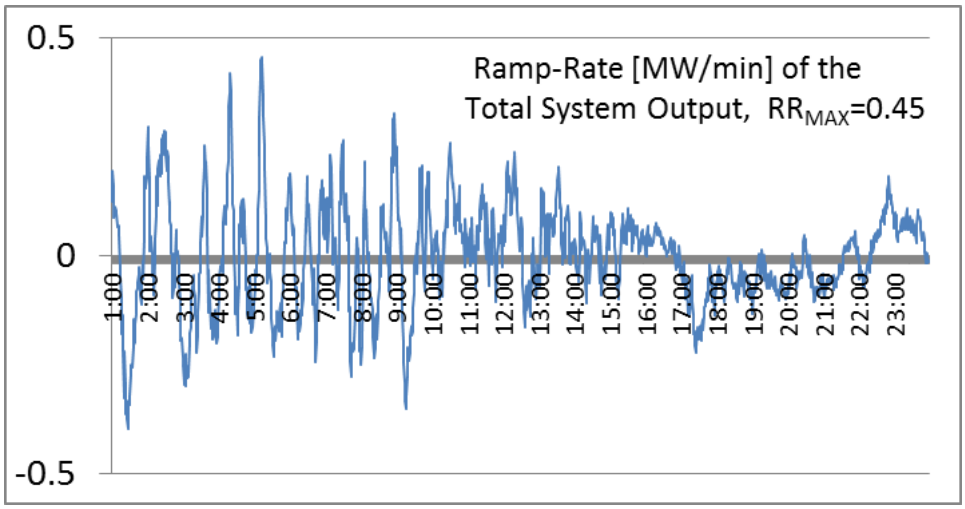

Figure 4.8 Ramp rate of total system power

The ramp rate of the total output power (TOP) in MW/min is expressed as

$$RR(t) = TOP(t) - TOP(t - 1\ \text{min}) \tag{4.4}$$

Figure 4.8 is a plot of the ramp rate corresponding to the total output power plotted in Fig. 4.7. As is evident in Fig. 4.8, the ramp rate of the total output power is less than 0.5 MW/min and thus easily satisfies the maximum ramp rate requirement of ±1 MW/min applied to the Kahuku wind farm.

Figure 4.9 presents SOC variations obtained using Eq. (2.4) under the assumption that a 1 MWh ultracapacitor was used for the A section. As is evident in Fig. 4.9, the maximum SOC is approximately 160%. This means that an ultracapacitor with at

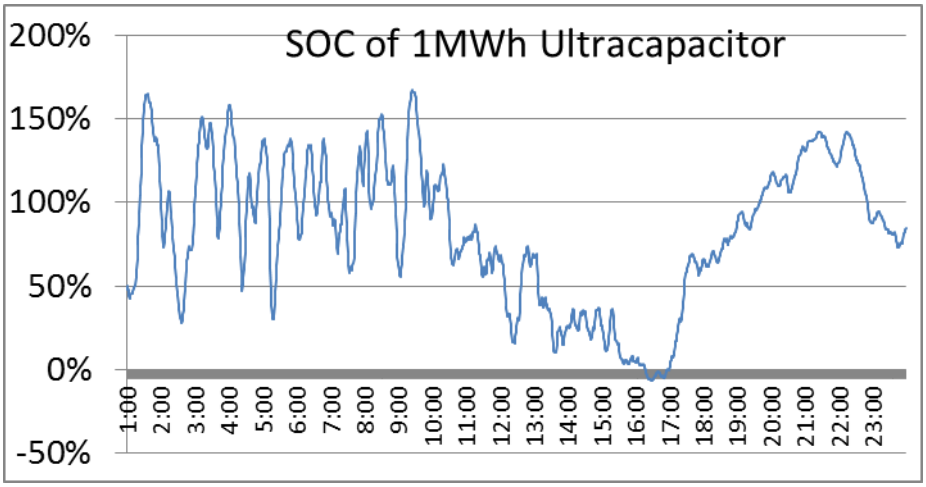

Figure 4.9 Time domain plot of the SOC for the A section of the wind farm output frequencies (see Fig. 4.4)

least 1.6 MWh capacity is needed. As shown in Table 2.2, the C-rate of an ultracapacitor can be as high as 200C. This high C-rate makes ultracapacitors feasible for use in an ES system for absorbing short-duration subway regenerative braking energy, as mentioned in chapter 2 [16]. In other words, during 30 s of subway braking, the ES system could absorb all of the regenerative braking energy. In addition, the ultracapacitor would provide the same performance when discharging this stored energy during 30 s of acceleration.

SOC correction can be carried out, as described in Section 3 of Chapter 2, in order to reduce the required capacity of the ultracapacitor to less than 1.6 MWh while effectively utilizing the high C-rate offered by the ultracapacitor. This SOC correction produces the results plotted in Fig. 4.10. From Fig. 4.10, it is readily apparent that the SOC after correction deviates less from the 50% level. In this case, the ultracapacitor exhibits energy neutral operation, with more frequent charging and discharging. The maximum SOC is approximately 75%, and the minimum SOC is approximately 20%.

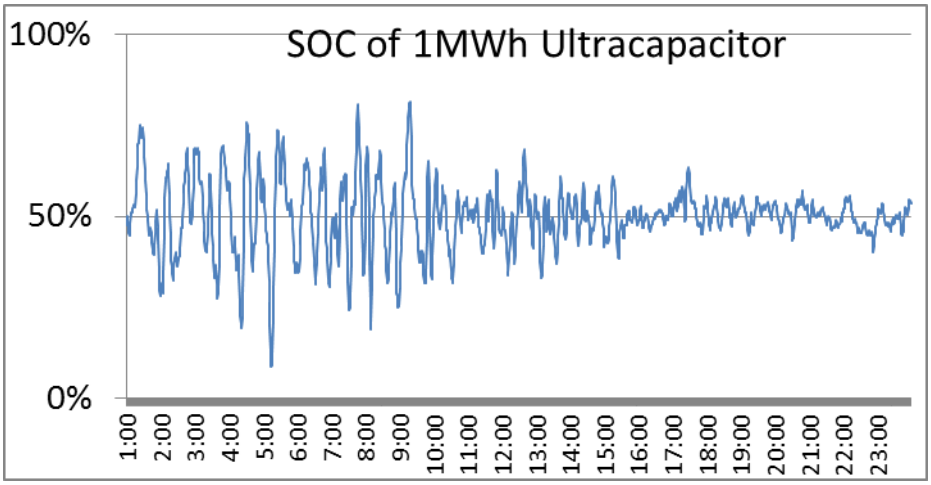

Figure 4.10 SOC after correction (with CIF = 1) corresponding to the SOC variations in Fig. 4.9

With SOC correction, the required capacity of 1.6 MWh corresponding to the data in Fig. 4.9 can be reduced to approximately 0.8 MWh.

It is very important to note that this type of SOC correction can negatively affect the targeted total system output (see Fig. 4.7), as mentioned in section 3 of chapter 2. Therefore, it is necessary to minimize the energy capacity of storage systems while satisfying the maximum ramp rate requirement of ±1 MW/min by appropriately adjusting the CIF values for the ultracapacitor and the LiB.

4.3 Repetitive Analysis for Effective Ramp Rate Control Using CIF Tuning

When the CIF of the ultracapacitor and the LiB are zero, the storage outputs are as shown in Figs. 4.5 and 4.6, respectively. After controlling the ramp rate with the HES system, the maximum ramp rate (RR_{MAX}) of the total output was 0.45 MW/min; this is significantly lower than the requirement of 1 MW/min, indicating some degree of inefficiency in the system. If the analysis is performed repeatedly with increasing CIF

values, more efficient operation can be achieved by reducing the capacity of the HES such that RR_{MAX} is closer to the maximum allowable value.

Table 4.2 presents the results of the repeated analyses. Figure 4.11 is a screen image of the user interface (created using Microsoft Excel) that was used to facilitate the process of repeatedly performing the analysis. The up- and down-arrow buttons increase or decrease CIF by 0.01 for each click. The results in the sixth row (indicated by boldface text) correspond to the most appropriate values. In the results in the seventh row, the energy capacity of the storage devices has been reduced too much, because the maximum ramp rate of the system exceeds the 1 MW/min requirement.

10 MW/1 MWh Ultracapacitor + 10 MW/10 MWh LiB System

CIF_{UC}	**CIF_{LiB}**	**SOC_{MAX-UC} [%]**	**P_{MAX-UC}** [MW]	**$SOC_{MAX-LiB}$ [%]**	**$P_{MAX-LiB}$** [MW]	**Total output RR_{MAX}** [MW/min]
0	0	167	8.8	84	8.8	0.45
0.05	0.05	151	8.7	89	8.9	0.61
0.1	0.1	139	8.6	90	8.9	0.76
0.12	0.2	135	8.5	83	8.8	0.84
0.15	0.3	130	8.3	76	8.8	0.93
0.17	**0.35**	**127**	**8.2**	**73**	**8.7**	**0.99**
0.18	0.36	126	8.2	73	8.7	1.02
0.2	0.5	123	8.1	70	8.7	1.10

Table 4.2 Repeated analyses of the HES with CIF tuning

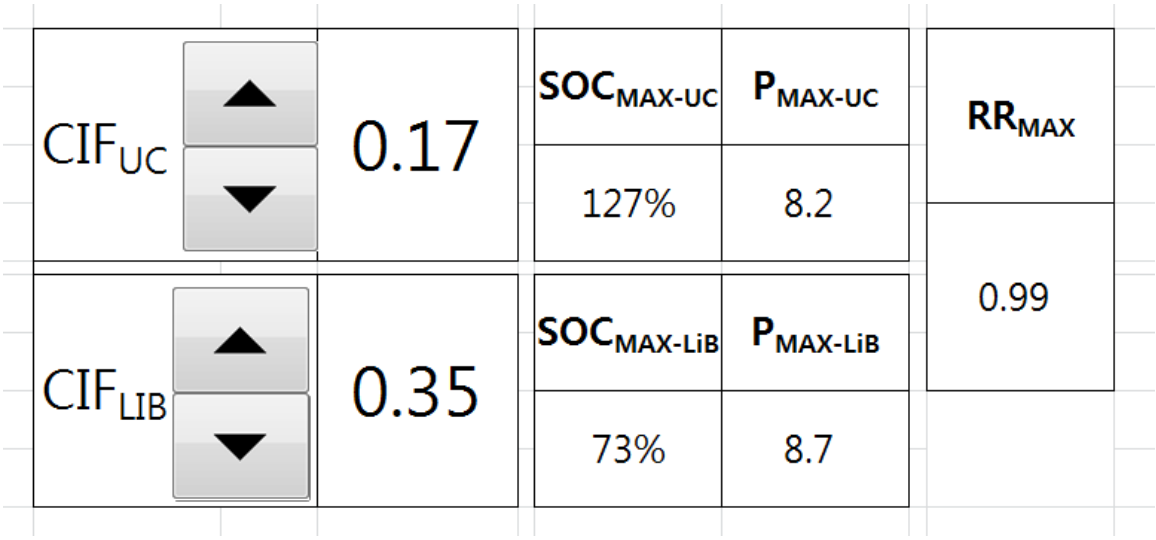

Figure 4.11 User interface for conveniently repeating the analysis of the HES while adjusting CIF values

The data in the sixth row indicate that an ultracapacitor capacity of at least 1.27 MWh is required because $SOC_{MAX\text{-}UC}$ is 127% of 1 MWh. In addition, the maximum power of the ultracapacitor PCS must be 8.2 MW. $SOC_{MAX\text{-}LiB}$ is 73% of 10 MWh, and thus the capacity of the LiB must be at least 7.3 MWh. The maximum power required for the LiB PCS is 8.7 MW. Table 4.3 presents the specifications and cost for an HES system based on the optimized values in the sixth row of Table 4.2.

	ES Type	**PCS Power**	**Battery Energy**	**Required C-rate**	**Cost**
Hybrid Energy Storage	Ultracapacitor	8.2MW	1.27MWh	6.5	27.9m$
	LiB	8.7MW	7.3MWh	1.2	10m$

Table 4.3 Optimized HES system that satisfies the maximum allowable ramp rate requirement of 1 MW/min

Chapter 5 Conclusion and Future Work

When the specifications given in Table 4.3 are compared to the actual 15 MW/10 MWh ES system manufactured by Xtreme Power for ramp control of the 30 MW Kahuku wind farm (see References [14] and [15]), it can be stated that the simulation generated acceptable results that are consistent with this real-life system.

In this thesis, the analysis was based on the 1-min-interval power profile of a wind farm from only one day. The output profile would exhibit significant variations according to the season and weather conditions, and thus it would be necessary to incorporate output profiles from multiple days to achieve a more accurate analysis.

Although the result values were reasonably produced, the biggest drawback of this simulation was that a systematic optimization method was not used. The most fundamental variables of analysis are diversity of real one day wind power profile, cutoff frequency that divides sections in the FFT result, and RR requirement. In addition, there are various variables that have to be handled through optimization, such as P_{LiB}, P_{UC}, E_{LiB}, E_{UC}, $CIF_{UC,}$ $CIF_{LiB,}$, and SOCs. Thus, although an enormous system might be needed to create an optimization program, there definitely is a need for challenge to make a progress in the manual method through repetition, which has a low accuracy. Furthermore, in future work it will be necessary to enhance the methodology of this thesis by including a more developed theoretical foundation and verifying the methodology through practical implementation.

References

[1] Jay Apt “The spectrum of power from wind turbines,” Journal of Power Sources., vol. 169, pp. 369-374, Feb. 2007

[2] F. Ahmadkhanlou and A. Goodarzi “Hybird lithium-ion/ultracap energy stroage systems for plug-in hybrid electric vehicles” Vehicle Power and Propulsion Conference(VPPC) IEEE, Sep. 2011

[3] M.A.Tankari and M.B.Camara “Wind power integration in hybrid power system active energy management” Ecologic Vehicles Renewable Energies(Monaco), Mar.2009

[4] H. Ibrahim and A Ilinca “Thchno-econimic analysis of different energy storage technologies” InTech 2013

[5] M. Cao, Q. Xu and P. Zeng “An energy storage system configuration method to stabilize power fluctuation in different operation periods” PES General Meeting Conference & Exposition IEEE 2014

[6] Y.V.Makarov, M. Kintner-Meyer, P. Du “Sizing Energy Storage to Accommodate High Penetration of Variable Energy Resources” Sustainable Energy IEEE Transactions, vol.3, Jan. 2012

[7] G. Mandic “Lithium-Ion Ultracapacitor Energy Stroage Integrated with a Variable Speed Wind Turbine for Improved Power Conversion Control” Ph.D.dissertation, UW Milwaukee, Dec. 2012

[8] J. Xiao and L. Bai “Sizing of Energy Storage and Diesel Generators in an Isolated Microgrid Using Discrete Fourier Transform” IEEE Transactions on Sustainable Energy, Vol. 5 July 2014

[9] M. Kintner-Meyer “Energy Storage for Power Systems Application: A Regional Assessment for the Northwest Power Pool(NWPP)” Pacific Northwest National Laboratory Apr. 2010

[10] M. Pedram and N. Chang “Hybrid Electrical Energy Storage Systems” ISLPED’10, Aug 2010

[11] C. Luo and B. Ooi “Frequency Deviation of Thermal Power Plants Due to Wind Farms” IEEE Transactions on Energy Conversion, vol.21, Sep. 2006

[12] C. Luo and H. Banakar “Strategies to Smooth Wind Power Fluctuations of Wind Turbine Generator” IEEE Transaction on Energy Conversion, vol.22, Jun 2007

[13] S. Teleke and M. Baran "Validation of Battery Energy Storage Control for Wind Farm Dispatching" Power and Energy Society General Meeting IEEE, 2010

[14] Xtreme Power Inc. "Xtreme Power's Dynamic Power Resource Online at Kahuku Wind(15MW project with first wind represents largest energy storage system integrated with a wind farm in north America)" www.xtremepower.com press release, Mar. 2011

[15] V.Gevorgian and D. Corbus "Ramping Performance Analysis of the Kahuku Wind-Energy Battery Stroage System" National Renewable Energy Laboratory(NREL) report, Nov. 2013

[16] K. Kim, "Subway Regenerative Brake Energy Storage Technology of Line No.2 of the Seoul Metro" Workshop of Energy Storage Technology, Feb. 2012

[17] S. Lim, "Large-Scale NaS Battery for Energy Storage" Workshop of Energy Storage Technology, 2012

[18] J.C. Zuleta "Who Will Win the Lithium-Ion Battery War?" Online Resource, Dec 2013

[19] A. Esmaili and A. Nasiri "Power Smoothing and Power Ramp Control for Wind Energy Using Energy Stroage" Energy Conversion Congress and Exposition IEEE, 2011

[20] J. P. Barton and D. G. Infield "Energy Stroage and Its Use with Intermittent Renewable Energy" IEEE Transaction on Energy Conversion, vol 19, Jun 2004

[21] I. Buchmann "BU-402: What is the C-rate" Online Resource, batteryuniversity.com, 2015

[22] MIT Electric Vehicle Team "A Guide to Understanding Battery Specifications" Online Resource, web.mit.edu, Dec. 2008.

[23] S. Min and S. Kim "Optimized Installation and Operations of Battery Energy Storage System and Electric Double Layer Capacitor Modules for Renewable Energy Based Intermittent Generation" JEET 2013.

[24] MathWorks Company "Matlab Fundamentals Online Self-paced Training" www.mathworks.com, 2014